Available online at www.sciencedirect.com
SCIENCE DIRECT®
ELSEVIER
Earth and Planetary Science Letters 216 (2003) 603–617
EPSL
www.elsevier.com/locate/epsl

High-pressure partial melting of garnet pyroxenite: possible mafic lithologies in the source of ocean island basalts

Tetsu Kogiso [a,b,c,*], Marc M. Hirschmann [a], Daniel J. Frost [b]

[a] *Department of Geology and Geophysics, University of Minnesota, Minneapolis, MN 55455, USA*
[b] *Bayerisches Geoinstitut, Universität Bayreuth, D-95440 Bayreuth, Germany*
[c] *Institute for Frontier Research on Earth Evolution, Japan Marine Science and Technology Center, Yokosuka 237-0061, Japan*

Received 13 March 2003; received in revised form 5 September 2003; accepted 17 September 2003

Abstract

Many ocean island basalts (OIB) that have isotopic ratios indicative of recycled crustal components in their source are silica-undersaturated and unlike silicic liquids produced from partial melting of recycled mid-ocean ridge basalt (MORB). However, experiments on a silica-deficient garnet pyroxenite, MIX1G, at 2.0–2.5 GPa show that some pyroxenite partial melts are strongly silica-undersaturated [M.M. Hirschmann et al., Geology 31 (2003) 481–484]. These low-pressure liquids are plausible parents of alkalic OIB, except that they are too aluminous. We present new partial melting experiments on MIX1G between 3.0 and 7.5 GPa. Partial melts at 5.0 GPa have low SiO_2 (<48 wt%), low Al_2O_3 (<12 wt%) and high CaO (>12 wt%) at moderate MgO (12–16 wt%), and are more similar to primitive OIB compositions than lower-pressure liquids of MIX1G or experimental partial melts of anhydrous or carbonated peridotite. Solidus temperatures at 5.0 and 7.5 GPa are 1625 and 1825°C, respectively, which are less than 50°C cooler than the anhydrous peridotite solidus. The liquidus temperature at 5.0 GPa is 1725°C, indicating a narrow melting interval ($\sim$100°C). These melting relations suggest that OIB magmas can be produced by partial melting of a silica-deficient pyroxenite similar to MIX1G if its melting residue contains significant garnet and lacks olivine. Such silica-deficient pyroxenites could be produced by interaction between recycled subducted oceanic crust and mantle peridotite or could be remnants of ancient oceanic lower crust or delaminated lower continental crust. If such compositions are present in plumes ascending with potential temperatures of 1550°C, they will begin to melt at about 5.0 GPa and produce appropriate partial melts. However, such hot plumes may also generate partial melts of peridotite, which could dilute the pyroxenite-derived partial melts.

Keywords: experimental petrology; partial melting; pyroxenite; mantle heterogeneity; alkali basalt

1. Introduction

Many ocean island basalts (OIB) have isotopic and trace element signatures that are believed to originate in ancient subducted mafic (clinopyroxene-rich) lithologies (e.g., [2,3]). However, experimentally derived partial melts of oceanic crustal

* Corresponding author. Mailing address: Department of Earth and Planetary Sciences, Tokyo Institute of Technology, Meguro, Tokyo 152-8551, Japan. Tel.: +81-3-5734-2338; Fax: +81-3-5734-3538.
E-mail address: kogisot@jamstec.go.jp (T. Kogiso).

0012-821X/03/$ – see front matter © 2003 Elsevier B.V. All rights reserved.
doi:10.1016/S0012-821X(03)00538-7

lithologies, namely quartz or coesite eclogites, are invariably silica-saturated (i.e., hypersthene- or quartz-normative) [4–6], and the same is undoubtedly true for mantle lithologies derived from subducted sediments or continental crust. In contrast, OIB with strong signatures of recycled components are typically silica-undersaturated (i.e., nepheline-normative) alkali basalts, basanites, and nephelinites (e.g., [1,7]). Clearly, subducted silica-saturated eclogite cannot be the direct source of such OIB. Understanding the petrogenesis of alkalic OIB is therefore of considerable interest in constraining the origin and history of the extreme isotopic heterogeneities sampled by many oceanic basalts.

The petrogenetic processes responsible for silica-undersaturated lavas are poorly known, but most models invoke an origin from small-degree partial melts of peridotite in the presence of $CO_2 \pm H_2O$ (e.g., [8,9]). Such models are based chiefly on inverse experiments showing that characteristic alkalic lava compositions (olivine melilitite, olivine basanite) are close to multiple saturation with garnet peridotite mineral assemblages in the presence of large amounts (10–38 wt%) of CO_2–H_2O fluids [10–12]. But to date no forward

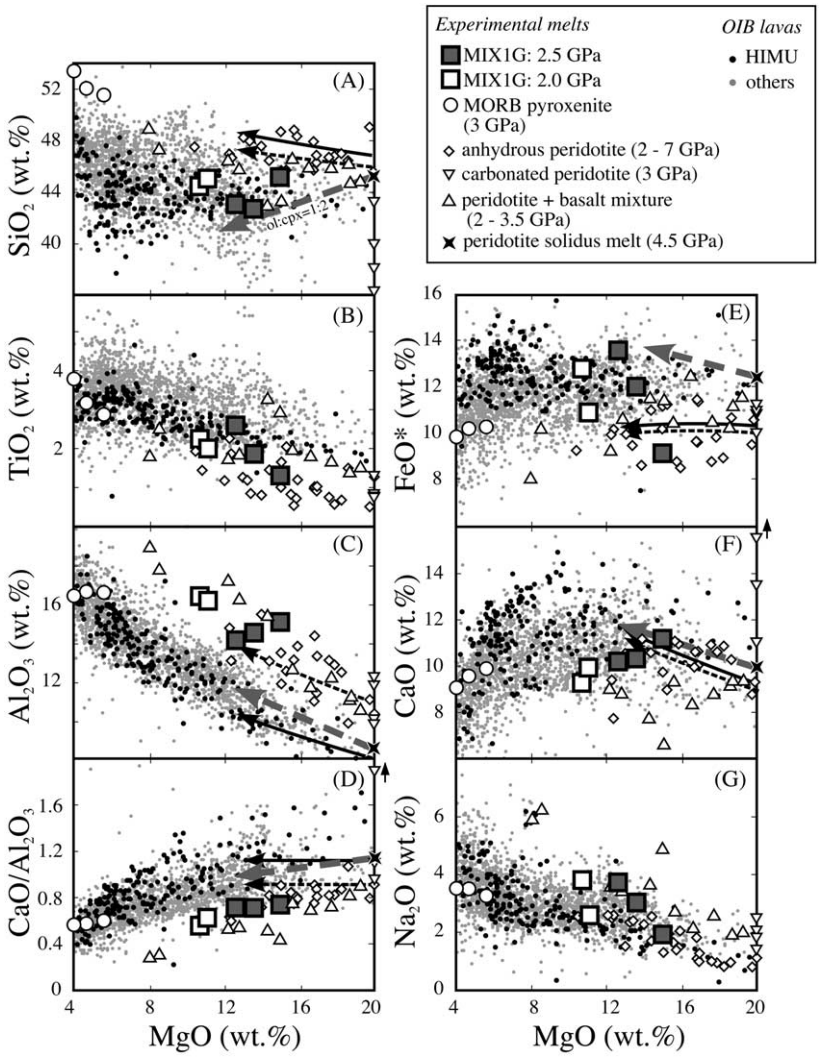

experiments have produced partial melts of peridotite that are plausible parents of alkalic OIB lavas (Fig. 1). This could be owing to the relative dearth of forward experiments involving peridotite+$CO_2 \pm H_2O$ that provide analyses of the liquids produced. It could also indicate that the inverse experiments do not provide an accurate guide to the origin of alkalic OIB, perhaps because their short durations (5–30 min) were not sufficient to achieve equilibrium.

An alternative hypothesis for the origin of silica-undersaturated OIB is derivation by partial melting of garnet pyroxenite [1]. Such pyroxenites may potentially provide a link between recycled crustal lithologies and the isotopic signatures evident in many OIB. Previous experiments on pyroxenite compositions have demonstrated that silica-undersaturated liquids can be produced from pyroxenite compositions [1,13], and some partial melts produced from a garnet pyroxenite (MIX1G) at 2.0–2.5 GPa are similar to alkalic OIB [1]. Although these liquids are too aluminous to be parental to OIB lavas, there is a negative correlation between Al_2O_3 and pressure (Fig. 1), suggesting that partial melts of MIX1G produced at higher pressure could be more similar to primitive alkalic OIB lavas than those produced at lower pressures. In this paper, we explore this premise via partial melting experiments on MIX1G between 3.0 and 7.5 GPa.

2. Compositions of alkalic OIB and their source lithologies

Compositions of mafic lavas from ocean islands that have strong isotopic signatures of the HIMU (high-μ), EM1 and EM2 mantle components are plotted in Fig. 1. There is considerable scatter in the data, which derive from a wide range of localities and analytical laboratories and which have not been filtered or corrected for the effects of alteration or crystal accumulation. Nevertheless, several key common characteristics are evident: (1) Primitive lavas are silica-poor, as expected for mafic rocks with significant normative nepheline; i.e., at 10 wt% MgO, most lie in the interval of 45 ± 3 wt% SiO_2 (Fig. 1A). (2) Variations in Al_2O_3 at a given MgO concentration are relatively small, with Al_2O_3 at 10 wt% MgO ranging between 11 and 13.5 wt% (Fig. 1C). (3) FeO* (total Fe as FeO) and CaO concentrations vary widely at a given MgO, but both range up to 14 wt%, most notably at islands with HIMU signatures (Fig. 1E,F). Here we consider whether these features of OIB can be explained by partial melting of peridotite or pyroxenite.

2.1. *Alkalic OIB from partial melting of peridotite?*

Strongly nepheline-normative liquids can be

←

Fig. 1. Compositions of mafic OIB lavas (MgO > 4 wt%) from selected ocean island chains with extreme (EM1, EM2, or HIMU) isotopic signatures (Azores, Canary, St. Helena, Tristan da Cunha, Marquesas, Pitcairn-Gambier, Society, Cook-Austral, and Samoa) from GEOROC database (http://georoc.mpch-mainz.gwdg.de/). Lavas from islands with extreme HIMU signatures (Mangaia, Rurutu, and Tubuai from Cook-Austral, and St. Helena) are shown by filled circles. Also shown are experimental partial melts of MIX1G garnet pyroxenite at low pressures (2.0–2.5 GPa) [1], G2 MORB-like pyroxenite (3.0 GPa) [6], anhydrous peridotite (2.0–7.0 GPa) [28,34,53], carbonated peridotite (3.0 GPa) [16], peridotite–pyroxenite mixtures (2.0–3.5 GPa) [5,17], and estimated composition of near-solidus partial melt of peridotite at 4.5 GPa ([18], C. Herzberg, personal communication). Carbonated peridotite partial melts are projected down to 20 wt% MgO along an olivine fractionation trend by assuming that $K_D^{Fe-Mg} = 0.35$. Thin arrows are olivine fractionation trends from representative high-pressure peridotite partial melts with compositions of MgO = 24 wt%, SiO_2 = 46.5 wt%, Al_2O_3 = 7 wt%, FeO* = 10 wt%, CaO = 8 wt% (thin solid arrows); and MgO = 20 wt%, SiO_2 = 46.5 wt%, Al_2O_3 = 10 wt%, FeO* = 10 wt%, CaO = 9 wt% (thin dashed arrows). Thick dashed arrows are fractionation trends of olivine and clinopyroxene (1:2 ratio in weight) at high pressures from the near-solidus melt of peridotite at 4.5 GPa. Clinopyroxene composition is taken from representative values of that in peridotite at 4.0–4.5 GPa [28]: MgO = 25 wt%, SiO_2 = 55 wt%, Al_2O_3 = 4 wt%, FeO* = 5 wt%, CaO = 10 wt%. Olivine fractionation of the more magnesian melt can produce liquids that intersect the distinctive Al_2O_3–MgO trend of OIB, but that are well above the SiO_2–MgO trend and below the FeO*–MgO trend of OIB. Fractionation of olivine and high-pressure clinopyroxene from near-solidus peridotite melt can explain OIB trends only when clinopyroxene/olivine ratios are as large as 2.

generated by small-degree partial melting of peridotite at high pressure [14], or of peridotite+$CO_2 \pm H_2O$ [15,16] or of peridotite hybridized by subducted basalt [5,17]. The latter mechanism is particularly appealing for genesis of alkalic OIB with strong signatures of recycling because it provides a link between the isotopic and petrologic character of these lavas. In fact, the low silica content of OIB from recycled sources could be explained by partial melting of a range of peridotite compositions. However, experimentally derived partial melts of peridotite, including anhydrous, volatile-rich, or hybridized varieties, do not match the MgO–Al_2O_3 or MgO–CaO characteristics of these OIB. Partial melts of various peridotites are richer in Al_2O_3 at a given MgO content than OIB (Fig. 1C). They also have lower CaO at a given MgO than many such OIB, and in particular than most OIB with strong HIMU signatures (Fig. 1F).

Fractionation of olivine from experimentally derived partial melts of volatile-poor peridotite or basalt–peridotite hybrids cannot yield liquids with all the compositional features of alkalic OIB. As shown in Fig. 1, such fractionation can produce liquids with MgO–Al_2O_3 systematics similar to some OIB, but with more SiO_2 than the lavas. On the other hand, because partial melts of peridotite+CO_2 have lower SiO_2 than CO_2-poor compositions (Fig. 1A), it is possible that fractionation of olivine from partial melts of carbonated peridotite ($\pm H_2O$) could match the MgO–SiO_2–Al_2O_3 systematics of alkalic OIB. However, as pointed out by Kogiso et al. [17], such a scenario fails to explain the relatively high FeO* of OIB (Fig. 1E). We emphasize that relatively few partial melt compositions of carbonated peridotite have been reported, but at this time there are no experiments that reproduce alkalic OIB compositions by peridotite partial fusion.

Herzberg and O'Hara [18] parameterized experimental data of peridotite partial melting and demonstrated that near-solidus partial melts of peridotite produced at 4–5 GPa can have high FeO* contents comparable to those of OIB (Fig. 1E). Such near-solidus melts could have as little as 8 wt% Al_2O_3 at 20 wt% MgO (C. Herzberg, personal communication, 2003), and olivine fractionation from such a liquid could potentially explain MgO–Al_2O_3 systematics of OIB lavas (Fig. 1C). However, inferred compositions of near-solidus partial melts of peridotite at 4–5 GPa are too SiO_2-rich to yield OIB lava trends by olivine fractionation alone (Fig. 1A). Crystallization of olivine and clinopyroxene at high pressures can produce low SiO_2 liquids from near-solidus peridotite melts, though explaining OIB trends requires that clinopyroxene crystallization exceeds that of olivine (Fig. 1). Because the phase volume of clinopyroxene shrinks relative to olivine with decreasing pressure (e.g., [19]), olivine crystallization dominates clinopyroxene in peridotite partial melts during mantle ascent. This makes it difficult to account for low SiO_2 contents of some OIB by clinopyroxene+olivine fractionation at high pressures. Clinopyroxene fractionation in crustal magma chambers may be an important process within OIB lava suites because trends on the MgO–Al_2O_3 and MgO–Al_2O_3/CaO plots cannot be produced by olivine fractionation alone (Fig. 1). Indeed, primitive alkalic OIB commonly contain clinopyroxene phenocrysts [7]. However, low-pressure clinopyroxene fractionation from the near-solidus peridotite melts cannot be principally responsible for OIB lava trends because the clinopyroxene crystallized at lower pressures has too much CaO (>20 wt% [7], T. Kogiso, unpublished data).

2.2. *Alkalic OIB from partial melting of pyroxenite?*

An alternative hypothesis for the genesis of alkalic OIB is that they derive from partial melts of pyroxenite. The existence of pyroxenite in OIB source regions has been inferred from the geochemistry of some OIB suites [20–24]. Many pyroxenites in the mantle may be *silica-deficient* [1], as considered in greater detail in Section 5, and these are capable of generating nepheline-normative partial melts.

Silica-deficient pyroxenites consist primarily of garnet and pyroxene, with minor amounts of other silica-poor minerals (olivine, spinel, and/or other oxides) [1]. In the pseudoternary system forsterite–Ca-Tschermaks pyroxene–quartz (Fo–CaTs–

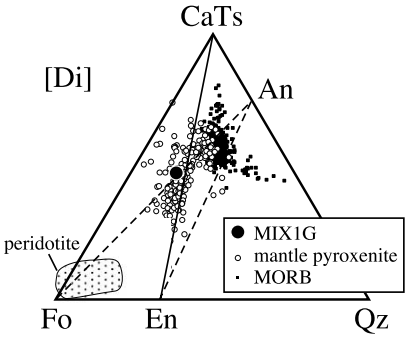

Fig. 2. Compositions of MIX1G starting material compared to mantle pyroxenites [35] in the pseudoternary system Fo–CaTs–Qz projected from Di, using the method of O'Hara [19]. Also plotted are MORB matrix glasses [40] and mantle peridotites [54]. Compositions plotting to the left of the Fo–An (anorthite) join are nepheline-normative, whereas those to the right of the join are hypersthene-normative or, if they plot to the right of the An–En (enstatite) join, quartz-normative. The CaTs–En join is a thermal divide for garnet pyroxenites. Those compositions plotting to the left of the join, such as MIX1G, will form partial melts that also plot to the silica-poor side of the divide. In most cases, these will also be nepheline-normative. In contrast, MORB plot to the right of the join and form silicic partial melts.

Qz) projected from diopside (Di) [19], such pyroxenites have less silica than the pyroxene (enstatite (En)–CaTs) join (Fig. 2). In contrast, rocks dominated by pyroxene and garnet that include minor amounts of quartz or other silica-rich phases are *silica-excess pyroxenites*. Previous partial melting experiments at 2.0 and 2.5 GPa on a silica-deficient garnet pyroxenite, MIX1G, produced strongly silica-undersaturated liquids [1]. These liquids have as high FeO* and CaO contents as alkalic OIB, although they have too high Al_2O_3 to be parental to OIB lavas (Fig. 1). Nevertheless, there is a negative correlation between Al_2O_3 and pressure (Fig. 1C), probably owing to enhanced garnet stability with increasing pressure. It can therefore be supposed that higher-pressure partial melts of MIX1G could be plausible parental liquids for alkalic OIB lavas.

3. Experimental procedures

The MIX1G starting material (Table 1) was constructed from natural mineral and rock powders [1] and was selected because it is an intermediate composition within the array of mantle pyroxenite. Experiments at 3.0 and 3.3 GPa were conducted using an end-loaded piston cylinder apparatus at the University of Minnesota and run procedures described in Kogiso and Hirschmann [13]. Experiments at 5.0 and 7.5 GPa were conducted between 1600 and 1850°C using a Walker-type multi-anvil apparatus at Universität Bayreuth. We used semi-sintered MgO/Cr_2O_3 octahedra with 18 mm edge length as pressure media, and WC cubes with 11 mm truncation edge length. The pressure was calibrated at 1000°C using the $CaGeO_3$ garnet to perovskite transformation at 6.1 GPa [25] and the SiO_2 coesite to stishovite at 8.7 GPa [26]. The furnace assembly consisted of a stepped $LaCrO_3$ heater with Mo electrodes at the ends, a ZrO_2 outer sleeve and MgO inner pieces. Sample powder was packed in a graphite crucible (inner size: 0.5 mm height × 0.5 mm diameter) placed in a Pt outer capsule. The assembled octahedra, furnace parts and sample capsule were stored in a vacuum oven overnight at 260°C before an experiment. We investigated the thermal gradient in our assembly at 7.5 GPa and 1500°C using an enstatite–diopside mixed powder and two-pyroxene thermometry from Nickel et al. [27]. The temperature difference across the sample position was found to be less than 50°C.

Table 1
Compositions (wt%) of starting material and MORB-like pyroxenite

	MIX1G[a]	G2[b]
SiO_2	45.56	50.05
TiO_2	0.90	1.97
Al_2O_3	15.19	15.76
FeO*[c]	7.77	9.35
MnO	0.15	0.17
MgO	16.67	7.90
CaO	11.48	11.74
Na_2O	1.44	3.04
K_2O	0.04	0.03
Total	99.20	100.00
Mg#[d]	79.3	60.1

[a] Hirschmann et al. [1].
[b] Typical MORB [6].
[c] Total Fe as FeO.
[d] Molar Mg/(Mg+Fe) × 100.

Table 2
Experimental run conditions and phase assemblages

Run no.	P (GPa)	T (°C)	Duration (h)	Phase[a]
A325	3.0	1400	72	grt, cpx, ol, sp
A320	3.3	1400	62 ± 8[b]	grt, cpx, ol, sp
V154	5.0	1600	1.0	grt, cpx, FeTi
V162	5.0	1650	6.0	melt, grt, cpx
V161	5.0	1675	6.0	melt, grt, cpx
V157	5.0	1700	0.5	melt, grt
V158	5.0	1750	0.5	melt
V149	7.5	1700	6.0	grt, cpx, FeTi
V153	7.5	1800	8 min	grt, cpx, FeTi
V159	7.5	1850	5 min	melt, grt, cpx

[a] Abbreviations: grt = garnet, cpx = clinopyroxene, ol = olivine, sp = spinel, FeTi = Fe–Ti oxide.
[b] Run A320 was accidentally terminated by a power failure, and exact run duration was not recorded.

Compositions of quenched phases were determined using a JEOL JXA8900R electron microprobe at University of Minnesota and JEOL JXA8800 at Tokyo Institute of Technology. Analyses were done using a 15 kV, 10 nA beam and 20 s peak acquisition time for all elements. Analytical precisions of major oxides are better than 2% relative [13], and inter-laboratory differences are negligible (Table 3). Phase proportions were calculated by mass balance between the compositions of coexisting phases and the bulk composition using a linear least squares method. Residual sums of squares range from 0.03 to 0.29, indicating reasonable mass balances between analyzed phases and the starting bulk composition.

4. Experimental results

Experimental conditions and corresponding phase assemblages are listed in Table 2 and plotted in Fig. 3 along with the results of lower-pressure experiments on MIX1G from Hirschmann et al. [1]. Crystal sizes range from 1–10 μm in subsolidus runs to 10–50 μm in near-liquidus runs. Quenched melt in all above solidus runs were composed of fine-grained quench crystals. Melt pools large enough to analyze by the electron microprobe are present in experimental charges from 5.0 GPa at 1650°C and hotter. Compositions and proportions of melt and mineral phases of the 5.0 GPa charges are given in Table 3. In the 5.0 GPa charges, there are no correlations of melt and mineral compositions with position within the capsule. Garnet and clinopyroxene crystals show no detectable compositional zoning. Average relative errors of major oxides are ∼1% for Si, ∼2% for Al, ∼3% for Fe, and ∼2% for Mg and Ca (Table 3). These values are comparable to microprobe analytical uncertainty. Oxide totals of melt compositions in all charges are above 99 wt%, indicating that amounts of volatiles in the charges are negligible. Fe–Mg exchange coefficients ($K_D = (Fe/Mg)_{mineral}/(Fe/Mg)_{melt}$) are 0.42 ± 0.03 and 0.27 ± 0.03 for garnet and clinopyroxene, respectively (Table 3), both of which are within the range of those in high-pressure experiments [28,29].

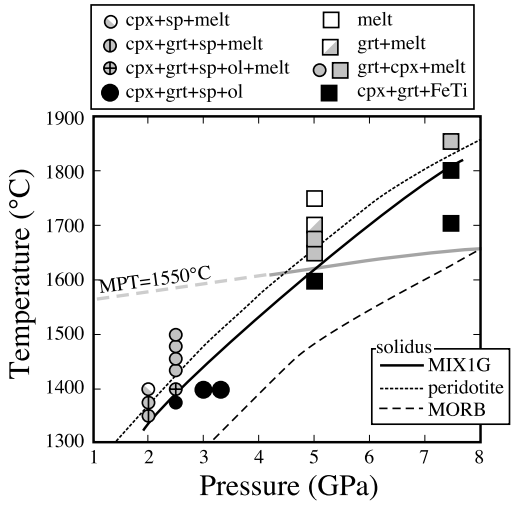

Fig. 3. Pressure–temperature diagram for partial melting experiments of MIX1G garnet pyroxenite. Data at 2.0 and 2.5 GPa (smaller symbols) are from Hirschmann et al. [1]. Larger circles and squares are, respectively, piston cylinder and multi-anvil data from this study. Solid curve is the estimated solidus of MIX1G, thin dashed curve is that of MORB [4] and dotted curve is that of typical peridotite [30]. An adiabatic path for mantle potential temperature (MPT) of 1550°C is also shown [55]. This MPT is approximately 200°C hotter than the oceanic ridge geotherm and is appropriate for hotspots such as Hawaii (e.g., [52]). Abbreviations: cpx = clinopyroxene, grt = garnet, sp = spinel, ol = olivine, FeTi = Fe–Ti oxide.

Table 3
Phase compositions (wt%) from 5.0 GPa experiments[a]

Run no.	Phase[b]	n[c]	SiO_2	TiO_2	Al_2O_3	FeO*	MnO	MgO	CaO	Na_2O	K_2O	Total	Mg#	Mode[d]	K_D[e]
V162	melt	8	46.75 (49)	3.13 (37)	6.38(39)	13.86(36)	0.14 (2)	13.39 (19)	13.60(29)	2.25 (14)	0.05 (4)	99.54	63.3	0.19	-
	grt	15	42.21 (29)	0.63 (5)	22.64(20)	7.66(19)	0.18 (2)	18.53 (25)	8.11(17)	0.07 (2)	0.01 (1)	100.04	81.2	0.53	0.40
	cpx	10	52.67 (33)	0.26 (4)	7.49(4)	4.44(15)	0.08 (2)	16.23 (16)	16.67(27)	2.01 (6)	0.00 (1)	99.85	86.7	0.28	0.26
V161	melt	11	47.35 (59)	1.93 (20)	10.15(51)	10.69(72)	0.17 (2)	13.59 (26)	12.80(31)	2.43 (16)	0.08 (4)	99.20	69.4	0.40	-
	grt	7	42.36 (19)	0.49 (7)	23.05(25)	6.65(23)	0.19 (4)	19.24 (28)	8.18(19)	0.06 (3)	0.00 (0)	100.24	83.8	0.43	0.44
	cpx	5	52.29 (33)	0.19 (2)	8.26(39)	3.84(6)	0.08 (3)	16.58 (19)	16.16(28)	1.93 (6)	0.02 (1)	99.35	88.5	0.17	0.30
V157	melt	9	46.99 (30)	1.13 (5)	12.49(13)	8.66(34)	0.16 (4)	15.32 (20)	12.47(13)	1.80 (10)	0.05 (2)	99.07	75.9	0.75	-
	grt	5	42.78 (22)	0.50 (3)	23.61(6)	5.00(17)	0.14 (5)	20.33 (15)	8.21(22)	0.06 (3)	0.00 (0)	100.63	87.9	0.25	0.44
UMN vs. TIT[f]															
	UMN	9	42.31 (30)	0.64 (5)	22.67(23)	7.53(9)	0.18 (3)	18.61 (28)	8.15(12)	0.07 (1)	0.01 (1)	100.17	81.5		
	TIT	6	42.05 (21)	0.63 (6)	22.60(16)	7.84(15)	0.18 (1)	18.42 (17)	8.06(23)	0.06 (2)	0.01 (1)	99.85	80.7		

[a] Numbers in parentheses are two standard deviations, and refer to the last digit(s).
[b] Phase abbreviations as in Table 2.
[c] Number of analyses.
[d] Weight fractions determined by mass balance calculations.
[e] Fe–Mg exchange coefficients (in mol) between mineral and melt: $(Fe/Mg)_{mineral}/(Fe/Mg)_{melt}$.
[f] Comparison of garnet compositions in V162 analyzed at University of Minnesota (UMN) and at Tokyo Institute of Technology (TIT).

4.1. Phase relations

The solidus is located between 1600 and 1650°C at 5.0 GPa and between 1800 and 1850°C at 7.5 GPa. At lower pressures, the solidus crosses 1400°C between 2.5 and 3.0 GPa (Fig. 3). Thus, the solidus of MIX1G garnet pyroxenite is probably less than 50°C lower than that of typical mantle peridotite within this pressure range estimated by Hirschmann [30], although both solidi could be indistinguishable within uncertainties in pressures of our experiments and of the peridotite solidus. The liquidus temperature is between 1700 and 1750°C at 5.0 GPa, indicating that the melting interval of MIX1G is as narrow as 100°C. A similarly narrow melting interval has been documented at these pressures for pyroxenite similar in composition to typical mid-ocean ridge basalt (MORB) [4].

The subsolidus mineral assemblage is garnet+clinopyroxene+olivine+spinel at $\leq$3.3 GPa, and garnet+clinopyroxene+an Fe–Ti oxide at 5.0 and 7.5 GPa. Owing to very small grain size (<1 μm), we are not able to identify the Fe–Ti oxide phase. Melt coexists with garnet and clinopyroxene near the solidus. At 5.0 GPa, the modal proportion of

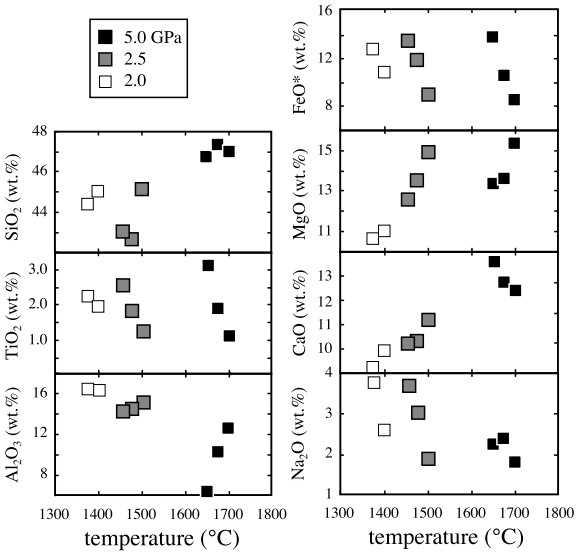

Fig. 4. Compositions of quenched melt from partial melting experiments of MIX1G garnet pyroxenite at 5.0 GPa (this study) and 2.0–2.5 GPa [1] plotted against run temperature.

garnet is larger than that of clinopyroxene and garnet is the liquidus phase (Table 3).

4.2. Melt composition

The melt compositions of 5.0 GPa experiments are plotted against temperature in Fig. 4, and against MgO contents and in the Fo–CaTs–Qz-normative diagram in Fig. 5. With increasing temperature, Al_2O_3 and MgO contents increase, TiO_2, FeO*, CaO and Na_2O contents decrease, and SiO_2 contents are nearly constant. The Na_2O content of the melt of the 1650°C run (V162) seems to be too low to balance the bulk composition (Table 3). This might be due to loss of some Na-bearing phases during polishing the

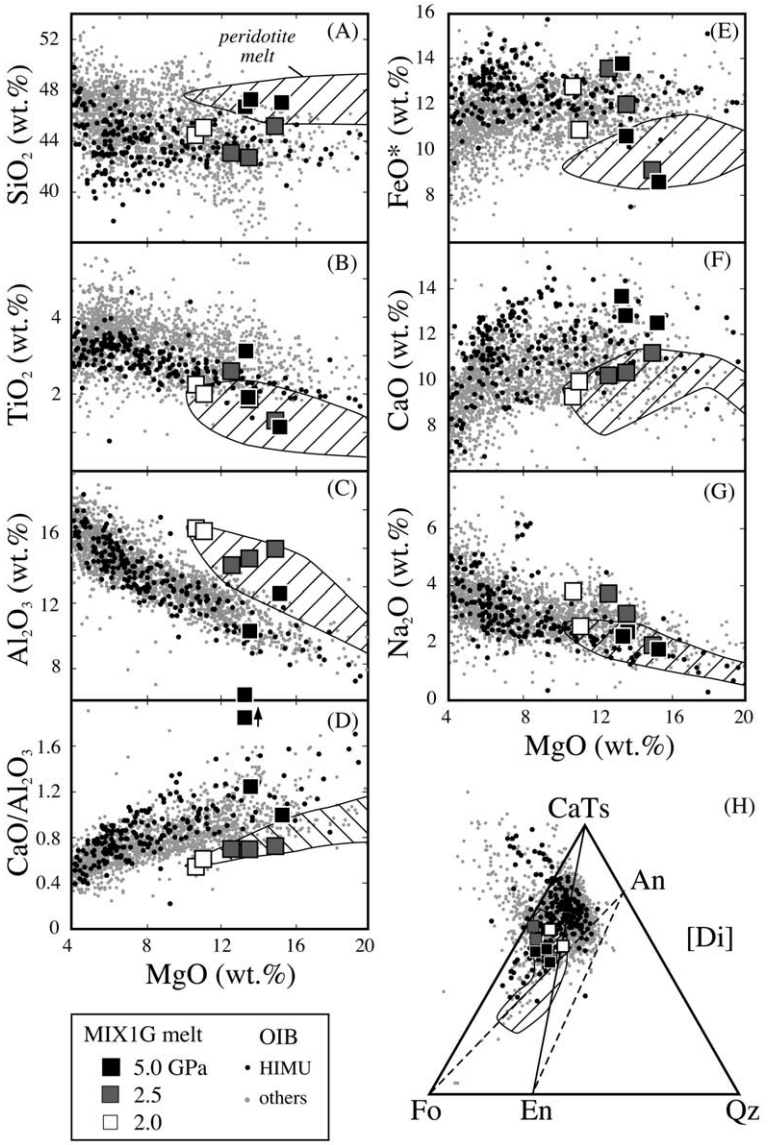

Fig. 5. Compositions of MIX1G partial melts compared to OIB lavas and experimental partial melts of anhydrous peridotite plotted against MgO (A–G) and in the pseudoternary Fo–CaTs–Qz diagram projected from Di following the methods of O'Hara [19] (H). Data sources are as in Fig. 1.

charge, and the actual content could be higher. Although we cannot identify lost phases, they are not likely volatile-bearing because the oxide total of the V162 melt is close to 100% (Table 3). All compositions are nepheline-normative and plot in the silica-deficient (left) side of the thermal divide (Fig. 5). Compared with MIX1G melts produced at lower pressures [1], 5.0 GPa melts have lower Al_2O_3 and higher SiO_2 and CaO contents (Fig. 5). In contrast, MgO contents are similar to those of lower-pressure melts.

5. Discussion

5.1. Comparison to OIB

Partial melts of MIX1G generated between 2.0 and 5.0 GPa ([1] and this study) are strongly nepheline-normative and have MgO, TiO_2, FeO*, CaO and Na_2O contents comparable to those in primitive alkalic OIB lavas (Fig. 5). Whereas the low-pressure partial melts are richer in Al_2O_3 than plausible parents of OIB suites, those generated at 5.0 GPa have Al_2O_3 comparable to those of primitive OIB lavas (Fig. 5C). Although SiO_2 contents of the 5.0 GPa melts of MIX1G are too high to be parental to OIB lavas, the SiO_2 range of MIX1G melts produced at 2.5–5.0 GPa overlaps that of the majority of primitive OIB lavas (Fig. 5A), that is, MIX1G partial melting at pressures between 2.5 and 5.0 GPa can produce liquids quite similar to primitive OIB. In fact, the high-pressure partial melts of MIX1G are more similar to the major element compositions of primitive OIB lavas than any other experimentally derived partial melts yet reported are (Figs. 1 and 5).

It is notable that the CaO contents of partial melts of MIX1G at 5.0 GPa are as high as those found in OIB with strong HIMU signatures, such as from St. Helena and the Cook-Austral islands (Fig. 5F). Such OIB are richer in CaO at a given MgO than other OIB [7] and than partial melts of anhydrous peridotite or peridotite–basalt mixtures (Fig. 1F). An alternative explanation for the high CaO in OIB with strong HIMU signatures is derivation from carbonated peridotite (Fig. 1F), but as mentioned above, such a mechanism may not be easily reconciled with the high FeO* of these lavas (Fig. 1E). Regardless, an adequate model for the HIMU source must explain the major element composition of the lavas as well as the trace element and isotopic characteristics of the HIMU reservoir. Relative to OIB lacking HIMU signatures, the sources of HIMU may contain a higher proportion of garnet pyroxenite like MIX1G or carbonated peridotite, but the former provides a better match to observed major elements (Figs. 1 and 5) and also may more easily be related to the recycled isotopic signatures that characterize HIMU.

5.2. Phase relations and production of OIB parental magmas

The decrease in Al_2O_3 in partial melts of pyroxenite observed with increasing pressure is a consequence of increasing stability of garnet relative to clinopyroxene. At low pressure (2.0–2.5 GPa), garnet disappears at lower temperature than clinopyroxene and spinel (Fig. 3), and more impor-

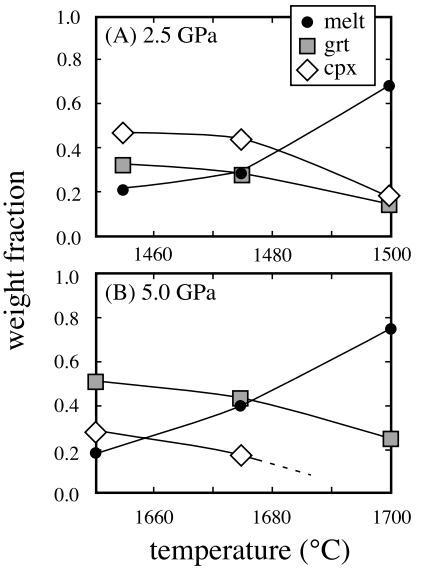

Fig. 6. Weight fractions of melt and residual mineral phases determined by mass balance calculations at 2.5 GPa (A: [1]) and 5.0 GPa (B: this study) plotted against run temperature. Note the increased stability of garnet with increasing pressure.

tantly, is always subordinate in abundance to clinopyroxene (Fig. 6A). In contrast, garnet is the liquidus phase at 5.0 GPa, and its mode is greater than that of clinopyroxene through the melting interval (Fig. 6B). As the stability field of garnet expands relative to clinopyroxene with increasing pressure, the Al_2O_3 contents of cotectic liquids decrease, and the CaO contents increase (Figs. 4 and 7).

It is important to note that olivine is a relatively minor factor in the phase equilibria of garnet pyroxenite, and consequently liquids do not vary greatly in MgO concentrations. Olivine has

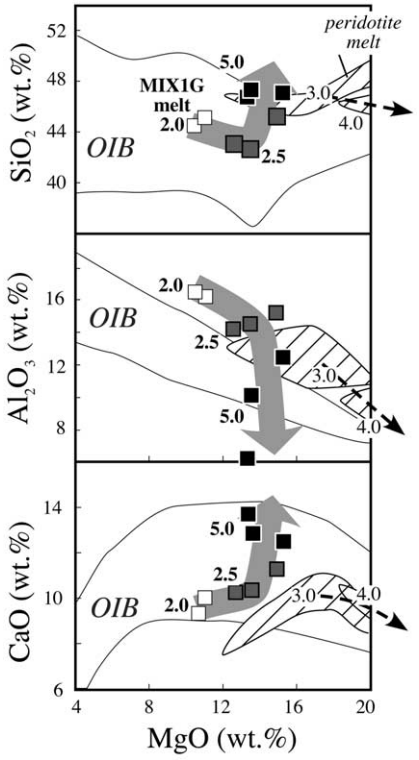

Fig. 7. Change in composition of partial melts of MIX1G garnet pyroxenite and anhydrous peridotite with increasing pressure. Numbers indicate pressures in GPa. With increasing pressure, partial melts of both lithologies diminish in Al_2O_3, owing to the increasing stability of garnet. However, MgO contents of MIX1G partial melts do not increase significantly with increasing pressure because of the absence of appreciable olivine in the residue, whereas partial melts of peridotite become enriched in MgO with increasing pressure owing to the dominant influence of the shrinking phase volume of olivine [28,34,53].

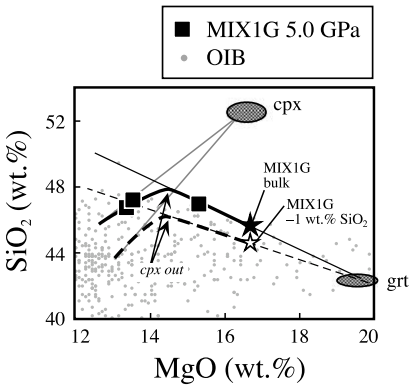

Fig. 8. MgO–SiO_2 systematics of pyroxenite partial melts. Thick solid curve indicates isobaric melting trend of MIX1G at 5.0 GPa. Once clinopyroxene is exhausted in the solid residue, the melt composition lies on the garnet control line (thin solid line). The same melting relation is expected to be maintained in partial melting of a pyroxenite similar to MIX1G but with less SiO_2 (thick dashed curve and thin dashed line). Such a SiO_2-depleted pyroxenite can produce partial melts with low SiO_2 contents that are more similar to primitive OIB lavas than MIX1G melts.

not been observed in the melting interval above 5.0 GPa (Fig. 3) and is present only in small amounts near the solidus at lower pressures (Fig. 3). Consequently, shifts in Al_2O_3 and CaO of MIX1G partial melts with increasing pressures are not accompanied by appreciable increases in MgO contents (Fig. 7).

Expansion of the garnet stability field at higher pressure also increases SiO_2 contents of partial melts because garnet is SiO_2-poor (Table 3, Fig. 7). As a result, partial melts of MIX1G at 5.0 GPa are too high in SiO_2 to be parental to OIB magmas (Fig. 5), although MIX1G melts produced between 2.5 and 5.0 GPa cover the wide range of SiO_2 contents of OIB lavas (Fig. 5A). It may be possible to produce liquids with much lower SiO_2 contents by partial melting from pyroxenites similar to MIX1G, but with slightly lower SiO_2 contents. Once clinopyroxene is exhausted in the solid residue during partial melting of a MIX1G-like pyroxenite at a given pressure, melt compositions lie along the garnet control line, as schematically illustrated in Fig. 8. Therefore, compositional trends of partial melts from a pyroxenite more depleted in SiO_2 than MIX1G would reach the garnet control line at lower

SiO_2 (Fig. 8), and consequently partial melts more depleted in SiO_2 are produced under similar P–T conditions. Note that such a SiO_2-depleted pyroxenite is expected to have a larger amount of garnet in its melting residue than MIX1G at similar degrees of melting because of its lower SiO_2 content (Fig. 8). This would result in partial melts more depleted in Al_2O_3 than those from MIX1G at the same P–T conditions, because Al_2O_3 contents of partial melts are principally controlled by garnet in the residue, as described above. Thus, a pyroxenite with less SiO_2 than MIX1G can produce partial melts with less SiO_2 and less Al_2O_3 contents, that is, liquids more similar to OIB parental liquids at similar or even higher degrees of melting.

Production of silica-undersaturated liquids from silica-deficient pyroxenite can be understood from consideration of the Fo–CaTs–Qz plot projected from Di (Figs. 2 and 5) [19]. The En–CaTs join of this projection is a thermal divide when garnet and pyroxene are sole minerals in the residue [19]. Therefore, silica-deficient garnet pyroxenites like MIX1G that plot on the silica-poor (left) side of the thermal divide generate silica-poor melts that also plot on the left side of the divide (Fig. 5H). Many are also nepheline-normative, such as the partial melts of MIX1G (Fig. 5H).

In summary, liquids parental to OIB lavas must be low in Al_2O_3 and rich in CaO. Production of such magmas from partial melting of pyroxenite requires that the residual solids contain an adequate amount of garnet, and that olivine is absent above the solidus. Also, the silica-undersaturated character of OIB requires that the pyroxenite bulk composition projects on the silica-deficient side of the thermal divide in the Fo–CaTs–Qz projection (Fig. 2). Our experiments demonstrate that MIX1G meets these requirements, but other pyroxenites with less SiO_2 that meet the above requirements could be better potential sources for silica-undersaturated OIB lavas. In addition, carbonated garnet pyroxenite may produce liquids with appropriate characteristics at temperatures well below those required for volatile-poor MIX1G.

The effect of pressure on partial melting relationships of peridotite is quite distinct from the effect on garnet pyroxenite. As is the case for pyroxenite, garnet becomes increasingly stable in peridotite with increasing pressure [28,31,32], leading to diminished Al_2O_3 in partial melts. But the dominant influence of the olivine phase volume on peridotite phase equilibria results in strongly increasing MgO of partial melts with increasing pressure [14,28,33,34]. Thus, in contrast to pyroxenite, high-pressure low Al_2O_3 partial melts of peridotite are very rich in MgO (i.e., they trend towards komatiite) (Fig. 7). In contrast, SiO_2 contents of peridotite partial melts are not greatly affected by pressure, because the effect of expansion of garnet stability on SiO_2 contents of partial melts has less leverage than buffering by olivine and pyroxene. Coexistence of garnet and olivine forces partial melts of peridotite to lie along a common trend in a plot of Al_2O_3 vs. MgO, but not in that of SiO_2 vs. MgO (Fig. 1). High-pressure partial melts of peridotite–MORB mixtures [17] are also buffered by garnet and olivine, and so plot along the same trend (Fig. 1). The same is true for partial melts of carbonated peridotite [16] (Fig. 1). Consequently, the MgO–SiO_2 and MgO–Al_2O_3 compositional fields of experimental peridotite melts and primitive OIB do not overlap (Figs. 1 and 5).

5.3. Origin of silica-deficient pyroxenite

Pyroxenites in the mantle may originate by many different processes [35], and as illustrated in Fig. 2, many pyroxenites from mantle samples are silica-deficient. However, pyroxenites sampled at the surface are not necessarily good analogs for those potentially present in basalt source regions in the convecting mantle, and so it is important to consider whether there are plausible processes to introduce significant silica-deficient pyroxenite into the source regions of OIB.

Subducted oceanic crust is the volumetrically dominant potential source of mantle pyroxenites, and most samples of modern oceanic crust, including virtually all MORB and most oceanic gabbros, have excess silica [36–40]. Nevertheless, oceanic crust may be converted to silica-deficient compositions by a combination of pro-

cesses in subduction zones and in the convecting mantle.

Dehydration of subducting oceanic crust likely extracts some or all of the free silica from descending quartz eclogite (e.g., [41]). If partial melting occurs, removal of siliceous liquids (e.g., [42]) would also reduce the silica content of the subducting residue. The result may be bimineralic pyroxenite, which consists solely of garnet and clinopyroxene. These plot along the thermal divide in the Fo–CaTs–Qz system (Fig. 2) and represent an intermediate case between silica-excess and silica-deficient pyroxenites.

Subducted oceanic crust is stretched and thinned by convective stirring of the mantle [43,44]. After ~1 Gyr, the typical thickness of recycled crust may be on the order of cm to a few meters [44]. Through a combination of mechanical and diffusive interactions with peridotite (e.g., [24,45–47]), these relatively thin bodies may become hybridized with surrounding peridotite, yielding olivine-bearing (and therefore silica-deficient) pyroxenite. Metasomatic silicate or carbonatite liquids may also promote this process. Note that hybridization can produce compositions suitable for generation of alkalic OIB by addition of a small amount of olivine, but extensive mixing between pyroxenite and peridotite would produce an olivine-rich lithology with melting relations similar to peridotite, and this would be less likely to produce partial melts with appropriate major element characteristics. For example, a 1:1 mixture of peridotite and MORB produces partial melts with compositions similar to partial melts of typical fertile peridotite (Fig. 1) [17]. Also, extensive interaction may yield pyroxenite with less radiogenic Os than observed in extreme OIB [24].

Oceanic gabbros with olivine more abundant than plagioclase on a molar basis are also silica-deficient, and though examples of such compositions are not abundant in modern oceanic crust [36–39], they may have been more common earlier in Earth history, when average oceanic crust compositions were probably more MgO-rich. The high MgO eclogites of Koidu, Sierra Leone may be examples of Archean silica-deficient lower oceanic crust [48]. Thus, a significant portion of ancient subducted oceanic crust may be silica-deficient.

Finally, there are plausible sources of silica-deficient mantle pyroxenite other than subducted oceanic crust and that may also carry extreme isotopic heterogeneities. For example, olivine-bearing pyroxene- or garnet-rich delaminated lower crust of continents or arcs [49] are expected to be silica-deficient and may be potential sources of the EM1 mantle reservoir [50]. Veins in the oceanic lithosphere, such as those invoked for the source central Atlantic islands with strong HIMU signatures [51] could also be silica-deficient; i.e., many of the pyroxenite xenoliths derived from the lithosphere beneath Hawaii, which may be reasonable analogs for such veins, are olivine-bearing and plot to the left of the thermal divide in the Fo–CaTs–Qz projection of Fig. 2.

5.4. Conditions of generation of alkalic OIB

Our experiments demonstrate that silica-deficient garnet pyroxenite similar to MIX1G can generate liquids parental to alkalic OIB near 5.0 GPa and 1650°C. However, it is not clear whether these are geodynamically reasonable conditions for generation of OIB. They require a mantle potential temperature ~200°C hotter than the oceanic geotherm (i.e., [52]) (Fig. 3) and would result in substantial peridotite partial melting if plumes ascend to the base of the lithosphere (~3 GPa, 100 km). Extensive contributions from peridotite would dilute the major element and isotopic signatures of pyroxenite partial melts. One possible resolution of this problem is partial melting of pyroxenite at lower temperature and pressure along less extreme geotherms, perhaps owing to modest amounts of $CO_2 \pm H_2O$, if appropriate compositions could be generated. Further experimental work is required to determine whether partial melts of carbonated silica-deficient pyroxenite can generate liquids that could be parental to alkalic OIB with strong signatures of recycling.

6. Conclusions

The solidus temperature of MIX1G, a silica-de-

ficient garnet pyroxenite, is <50°C lower than that of typical mantle peridotite over the pressure range of 3.0–7.5 GPa. At 5.0 GPa, MIX1G produces low Al_2O_3, silica-undersaturated partial melts with many similarities to primitive OIB lavas with strong isotopic signatures of crustal recycling. Thus, garnet pyroxenite compositions similar to MIX1G may be plausible sources for parental liquids of OIB lavas. The phase relations of MIX1G in its melting interval suggest that mafic lithologies can be sources of OIB parental magmas if they (1) are silica-deficient relative to the garnet–clinopyroxene thermal divide in the Fo–CaTs–Qz system, (2) are relatively poor in olivine such that high-temperature high-pressure partial melts are not highly enriched in MgO and (3) produce partial melts that are low in Al_2O_3 owing to buffering by garnet. Such silica-deficient pyroxenites could be produced by interactions between recycled subducted oceanic crust and mantle peridotite. Alternatively, ancient lower oceanic crust or delaminated lower continental crust may be sources of silica-deficient pyroxenite in the convecting mantle.

Acknowledgements

We thank Dave Rubie for support for the high-pressure experiments. This paper benefited from constructive reviews by Paula Smith, Michael Walter, and Claude Herzberg. This work was supported by NSF grant OCE9876255 to M.M.H.*[BW]*

References

[1] M.M. Hirschmann, T. Kogiso, M.B. Baker, E.M. Stolper, Alkalic magmas generated by partial melting of garnet pyroxenite, Geology 31 (2003) 481–484.
[2] C.G. Chase, Oceanic island Pb: two-stage histories and mantle evolution, Earth Planet. Sci. Lett. 52 (1981) 227–284.
[3] A.W. Hofmann, W.M. White, Mantle plumes from ancient oceanic crust, Earth Planet. Sci. Lett. 57 (1982) 421–436.
[4] A. Yasuda, T. Fujii, K. Kurita, Melting phase relations of an anhydrous mid-ocean ridge basalt from 3 to 20 GPa: implications for the behavior of subducted oceanic crust in the mantle, J. Geophys. Res. 99 (1994) 9401–9414.
[5] G.M. Yaxley, D.H. Green, Reactions between eclogite and peridotite: mantle refertilisation by subduction of oceanic crust, Schweiz. Mineral. Petrogr. Mitt. 78 (1998) 243–255.
[6] M. Pertermann, M.M. Hirschmann, Partial melting experiments on a MORB-like pyroxenite between 2 and 3 GPa: constraints on the presence of pyroxenites in basalt source regions from solidus location and melting rate, J. Geophys. Res. 108 (2003) 2125, doi: 10.1029/2000JB-000118.
[7] T. Kogiso, Y. Tatsumi, G. Shimoda, H.G. Barsczus, High μ (HIMU) ocean island basalts in southern Polynesia: new evidence for whole-mantle scale recycling of subducted oceanic crust, J. Geophys. Res. 102 (1997) 8085–8103.
[8] A.D. Edgar, The genesis of alkaline magmas with emphasis on their source regions: inferences from experimental studies, in: J.G. Fitton, B.G.J. Upton (Eds.), Alkaline Igneous Rocks, Geol. Soc. Spec. Publ. 30, 1987, pp. 29–52.
[9] C. Hémond, C.W. Devey, C. Chauvel, Source compositions and melting processes in the Society and Austral plumes (South Pacific Ocean): Element and isotope (Sr, Nd, Pb, Th) geochemistry, Chem. Geol. 115 (1994) 7–45.
[10] D.H. Green, Experimental melting studies on model upper mantle compositions at high pressure under both water-saturated and water-undersaturated conditions, Earth Planet. Sci. Lett. 19 (1973) 37–53.
[11] G. Brey, D.H. Green, The role of CO_2 in the genesis of olivine melilitite, Contrib. Mineral. Petrol. 49 (1975) 93–103.
[12] G. Brey, D.H. Green, Systematic study of liquidus phase relations in olivine melilitite+H_2O+CO_2 at high pressures and petrogenesis of an olivine melilitite magma, Contrib. Mineral. Petrol. 61 (1977) 141–162.
[13] T. Kogiso, M.M. Hirschmann, Experimental study of clinopyroxenite partial melting and the origin of ultra-calcic melt inclusions, Contrib. Mineral. Petrol. 142 (2001) 347–360.
[14] E. Takahashi, I. Kushiro, Melting of a dry peridotite at high pressures and basalt magma genesis, Am. Mineral. 68 (1983) 859–879.
[15] D.H. Eggler, The effect of CO_2 upon partial melting of peridotite in the system Na_2O–CaO–Al_2O_3–MgO–SiO_2–CO_2 to 35 kb, with an analysis of melting in a peridotite–H_2O–CO_2 system, Am. J. Sci. 278 (1978) 305–343.
[16] K. Hirose, Partial melt compositions of carbonated peridotite at 3 GPa and role of CO_2 in alkali-basalt magma generation, Geophys. Res. Lett. 24 (1997) 2837–2840.
[17] T. Kogiso, K. Hirose, E. Takahashi, Melting experiments on homogeneous mixtures of peridotite and basalt: application to the genesis of ocean island basalts, Earth Planet. Sci. Lett. 162 (1998) 45–61.
[18] C. Herzberg, M.J. O'Hara, Plume-associated ultramafic

magmas of Phanerozoic age, J. Petrol. 43 (2002) 1857–1883.
[19] M.J. O'Hara, The bearing of phase equilibria studies in synthetic and natural systems on the origin and evolution of basic and ultrabasic rocks, Earth Sci. Rev. 4 (1968) 69–133.
[20] E.H. Hauri, Major-element variability in the Hawaiian mantle plume, Nature 382 (1996) 415–419.
[21] O. Sigmarsson, S. Carn, J.C. Carracedo, Systematics of U-series nuclides in primitive lavas from the 1730-36 eruption on Lanzarote, Canary Islands, and implications for the role of garnet pyroxenites during oceanic basalt formations, Earth Planet. Sci. Lett. 162 (1998) 137–151.
[22] J.C. Lassiter, E.H. Hauri, P.W. Reiners, M.O. Garcia, Generation of Hawaiian post-erosional lavas by melting of a mixed lherzolite/pyroxenite source, Earth Planet. Sci. Lett. 178 (2000) 269–284.
[23] E.H. Hauri, Osmium isotopes and mantle convection, Philos. Trans. R. Soc. Lond. A 360 (2002) 2371–2382.
[24] T. Kogiso, M.M. Hirschmann, P.W. Reiners, Length scales of mantle heterogeneities and their relationship to ocean island basalt geochemistry, Geochim. Cosmochim. Acta, in press (2003).
[25] J. Susaki, M. Akaogi, S. Akimoto, O. Shimomura, Garnet–perovskite transformation in $CaGeO_3$: in-situ X-ray measurements using synchrotron radiation, Geophys. Res. Lett. 12 (1985) 729–732.
[26] J. Zhang, B. Li, W. Utsumi, R.C. Liebermann, In situ X-ray observations of the coesite–stishovite transition: reversed phase boundary and kinetics, Phys. Chem. Miner. 23 (1996) 1–10.
[27] K.G. Nickel, G.P. Brey, L. Kogarko, Orthopyroxene–clinopyroxene equilibria in the system $CaO–MgO–Al_2O_3–SiO_2$ (CMAS): new experimental results and implications for two-pyroxene thermometry, Contrib. Mineral. Petrol. 91 (1985) 44–53.
[28] M.J. Walter, Melting of garnet peridotite and the origin of komatiite and depleted lithosphere, J. Petrol. 39 (1998) 29–60.
[29] K. Putirka, Clinopyroxene+liquid equilibria to 100 kbar and 2450 K, Contrib. Mineral. Petrol. 135 (1999) 151–163.
[30] M.M. Hirschmann, The mantle solidus: experimental constraints and the effect of peridotite composition, Geochem. Geophys. Geosyst. 1 (2000) 2000GC000070.
[31] E. Takahashi, Melting of a dry peridotite KLB-1 up to 14 GPa: implications on the origin of peridotitic upper mantle, J. Geophys. Res. 91 (1986) 9367–9382.
[32] J. Zhang, C. Herzberg, Melting experiments on anhydrous peridotite KLB-1 from 5.0 to 22.5 GPa, J. Geophys. Res. 99 (1994) 17729–17742.
[33] D.C. Presnall, S.A. Dixon, J.R. Dixon, T.H. O'Donnell, N.L. Brenner, R.L. Schrock, D.W. Dycus, Liquidus phase relations on the join diopside–forsterite–anorthite from 1 atm to 20 kbar; their bearing on the generation and crystallization of basaltic magma, Contrib. Mineral. Petrol. 66 (1978) 203–220.
[34] K. Hirose, I. Kushiro, Partial melting of dry peridotites at high pressures: determination of compositions of melts segregated from peridotite using aggregates of diamond, Earth Planet. Sci. Lett. 114 (1993) 477–489.
[35] M.M. Hirschmann, E.M. Stolper, A possible role for garnet pyroxenite in the origin of the 'garnet signature' in MORB, Contrib. Mineral. Petrol. 124 (1996) 185–208.
[36] J.D. Smewing, N.I. Christensen, I.D. Bartholomew, P. Browning, The structure of the oceanic upper mantle and lower crust as deduced from the northern section of the Oman ophiolite, in: I.G. Gass, S.J. Lippard, A.W. Shelton (Eds.), Ophiolites and Oceanic Lithosphere, Geol. Soc. Spec. Publ. 13, 1984, pp. 41–53.
[37] H.J.B. Dick, S.H. Bloomer, S.H. Kirby, D.S. Stakes, C.K. Mawer, Lithostratigraphic evolution of an in-situ section of oceanic layer 3, in: R.P. Von Herzen et al. (Eds.), Proc. Ocean Drill. Prog. Sci. Res. 118, 1991, pp. 439–538.
[38] K.M. Gillis, C. Mevel, J.F. Allan et al., Site 895, in: K.M. Gillis, et al. (Eds.), Proceedings of the Ocean Drilling Program, Part A: Initial Reports 147, 1993, pp. 109–157.
[39] R. Hekinian, D. Bideau, J. Francheteau, J.L. Cheminee, R. Armijo, P. Lonsdale, N. Blum, Petrology of the East Pacific Rise crust and upper mantle exposed in Hess Deep (eastern Equatorial Pacific), J. Geophys. Res. 98 (1993) 8069–8094.
[40] W.G. Melson, T. O'Hearn, P. Kimberly, Volcanic glasses from sea-floor spreading centers and other deep sea tectonic settings: Major and minor element compositions in the Smithsonian WWW Data Set (abstract), EOS Trans. AGU 80 (1999) F1177.
[41] C.E. Manning, The solubility of quartz in H_2O in the lower crust and upper mantle, Geochim. Cosmochim. Acta 58 (1994) 4831–4839.
[42] R.P. Rapp, E.B. Watson, Dehydration melting of metabasalt at 8–32 kbar; implications for continental growth and crust-mantle recycling, J. Petrol. 36 (1995) 891–931.
[43] C. Allègre, D.L. Turcotte, Implications of a two-component marble-cake mantle, Nature 323 (1986) 123–127.
[44] L.H. Kellogg, D.L. Turcotte, Mixing and the distribution of heterogeneities in a chaotically convecting mantle, J. Geophys. Res. 95 (1990) 421–432.
[45] U.R. Christensen, A.W. Hofmann, Segregation of subducted oceanic crust in the convecting mantle, J. Geophys. Res. 99 (1994) 19867–19884.
[46] D.L. Farber, Q. Williams, F.J. Ryerson, Diffusion in Mg_2SiO_4 polymorphs and chemical heterogeneity in the mantle transition zone, Nature 371 (1994) 693–695.
[47] A. Tabit, J. Kornprobst, A.B. Woodland, The garnet peridotites of the Beni Bousera Massif (Morocco): tectonic mixing and iron–magnesium interdiffusion, C. R. Acad. Sci. Ser. II Sci. Terre Planet. 325 (1997) 665–670.
[48] M.G. Barth, R.L. Rudnick, I. Horn, W.F. McDonough, M.J. Spicuzza, J.W. Valley, S.E. Haggerty, Geochemistry of xenolithic eclogites from West Africa, part II: origins of the high MgO eclogites, Earth Planet. Sci. Lett. 177 (2002) 287–300.
[49] M. Jull, P.B. Kelemen, On the conditions for lower crus-

tal convective instability, J. Geophys. Res. 106 (2001) 6423–6446.
[50] Y. Tatsumi, Continental crust formation by crustal delamination in subduction zones and complementary accumulation of the enriched mantle I component in the mantle, Geochem. Geophys. Geosyst. 1 (2000) 2000GC-000094.
[51] A.N. Halliday, D.-C. Lee, S. Tommasini, G.R. Davies, C.R. Paslick, J.G. Fitton, D.E. James, Incompatible trace elements in OIB and MORB and source enrichment in the sub-oceanic mantle, Earth Planet. Sci. Lett. 133 (1995) 379–395.
[52] D. McKenzie, M.J. Bickle, The volume and composition of melt generated by extension of the lithosphere, J. Petrol. 29 (1988) 625–679.
[53] I. Kushiro, Partial melting of a fertile mantle peridotite at high pressures: an experimental study using aggregates of diamond, in: A. Basu, S. Hart (Eds.), Earth Processes: Reading the Isotopic Code, Geophysical Monograph 95, American Geophysical Union, Washington, DC, 1996, pp. 109–122.
[54] C. Herzberg, M. Feigenson, C. Skuba, E. Ohtani, Majorite fractionation recorded in the geochemistry of peridotites from South Africa, Nature 332 (1988) 823–826.
[55] J. Ita, L. Stixrude, Petrology, elasticity, and composition of the mantle transition zone, J. Geophys. Res. 97 (1992) 6849–6866.